Development of a Dynamic Mooring Module FEAM for FAST v8

Texas A&M University

Table of Contents

The FEAM mooring module in FAST v8 calculate the mooring line restoring force at the fairlead position of the floating platform considering the inertia and drag forces at each line element. In FEAM module, the elastic rod model is used for modeling the mooring system. This model is ideal for small strain, large displacement structural analysis of slender members such as tether and catenary mooring lines. A single global coordinate system is used in the finite element formulation of the rod model. Therefore, the model is simpler and more efficient than other conventional nonlinear models, such as the updated Lagrangian beam model. Detailed theory and finite element modeling of the rod can be found in Nordgren (1974) and Garrette (1982). In FEAM module, the model was improved to include the stretch of the element under the axial tension.

1. Theory of Rod

This theory describes the behavior of slender rods in terms of the position of the centerline of the rod. As illustrated in Figure 1, a position vector $\mathbf{r}(s,t)$ is introduced to define the space curve, which is a function of arc length s and time t. If we assume that the rod is inextensible, then the unit tangent vector to the space curve is $\mathbf{r}'$, and the principal normal vector is directed along $\mathbf{r}''$ and the bi-normal is directed along $\mathbf{r}' \times \mathbf{r}''$ where the prime symbol represents the differentiation with respect to the arc length.
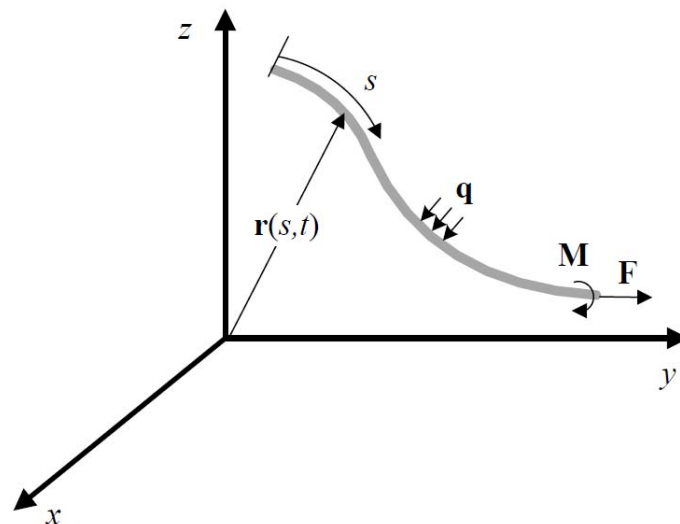

Figure 1. Coordinate system for slender rod

The equation of motion can be derived by equilibrium of the linear force and moment at the unit arc length of the rod as follows

$$\mathbf{F}' + \mathbf{q} = \rho\ddot{\mathbf{r}} \tag{1}$$

$$\mathbf{M}' + \mathbf{r}' \times \mathbf{F}' + \mathbf{m} = \mathbf{0} \tag{2}$$

where $\mathbf{q}$ is the applied force per unit length, ρ is the mass per unit length of the rod, $\mathbf{m}$ is the applied moment per unit length. $\mathbf{F}$ and $\mathbf{M}$ are the resultant force and moment along the centerline. The dot denotes the differentiation with respect to time.

The resultant moment $\mathbf{M}$ can be expressed as

$$\mathbf{M}' = \mathbf{r}' \times EI\mathbf{r}'' + H\mathbf{r}' \tag{3}$$

where EI is the bending stiffness, H is the torque. This relationship indicates that the bending moment is proportional to the curvature and is directed along the bi-normal direction. Substituting this relation into Equation (2), we have

$$\mathbf{r}' \times \left[\left(EI\mathbf{r}'' \right)' + \mathbf{F} \right] + H'\mathbf{r}' + H\mathbf{r}'' + \mathbf{m} = \mathbf{0} \tag{4}$$

and the scalar product of the above equation with $\mathbf{r}'$ yields

$$H' + \mathbf{m} \cdot \mathbf{r}' = \mathbf{0} \tag{5}$$

If we assume that there is no distributed torsional moment ($\mathbf{m} \cdot \mathbf{r}'$), and the torque in the lines is negligible, then the Equation (4) can be re-written as

$$\mathbf{r}' \times \left[\left(EI\mathbf{r}'' \right)' + \mathbf{F} \right] = \mathbf{0} \tag{6}$$

Introducing a scalar function $\lambda(s,t)$, which is called the Lagrangian multiplier, the $\mathbf{F}$ in the above equation can be written as

$$\mathbf{F} = -\left(EI\mathbf{r}''\right)' + \lambda\mathbf{r}' \tag{7}$$

The scalar product of Equation (7) with $\mathbf{r}'$ results in

$$\lambda = \mathbf{F} \cdot \mathbf{r}' - \left(EI\mathbf{r}''\right)' \cdot \mathbf{r}' \tag{8}$$

or

$$\lambda = T - EI\kappa^2 \tag{9}$$

where T is the tension and the κ is the curvature of the rod.

Combining Equation (7) with (1), the equation of motion for the rod become

$$-\left(EI\mathbf{r}''\right)'' + \left(\lambda\mathbf{r}'\right)' + \mathbf{q} = \rho\ddot{\mathbf{r}} \tag{10}$$

In addition, $\mathbf{r}$ should satisfy the inextensible condition as

$$\mathbf{r}' \cdot \mathbf{r}' = 1 \tag{11}$$

If the rod is extensible, and the stretch is linear and small, the above condition (11) can be approximated by

$$\frac{1}{2}\left(\mathbf{r}' \cdot \mathbf{r}' - 1\right) = \frac{T}{AE} \approx \frac{\lambda}{AE} \tag{12}$$

The above equation of motion of the rod and inextensible (or extensible) condition with initial and boundary conditions and applied force vector $\mathbf{q}$, are sufficient to determine the position vector $\mathbf{r}(s,t)$ and the Lagrangian multiplier $\lambda(s,t)$. The applied force vector $\mathbf{q}$, in most offshore applications, comes from the gravity of the rod and the hydrostatic and hydrodynamic forces from surrounding fluid. So it can be expressed as

$$\mathbf{q} = \mathbf{w} + \mathbf{F}^{\mathrm{s}} + \mathbf{F}^{\mathrm{d}} \tag{13}$$

where $\mathbf{w}$ is the weight of the rod per unit length, $\mathbf{F^s}$ is the hydrostatic force and $\mathbf{F^d}$ is the hydrodynamic force on the rod per unit length. The hydrostatic force can be written as

$$\mathbf{F^s} = \mathbf{B} - \left(P\mathbf{r'} \right)'$$

(14)

where $\mathbf{B}$ is the buoyancy force on the rod per unit length, and P is the hydrostatic pressure at point $\mathbf{r}$ on the rod. If a cross section area of the mooring line is small, then the hydrostatic pressure P can be neglected as programmed in FEAM module.

The hydrodynamic force $\mathbf{F^d}$ can be derived by Morison's formula below

$$\begin{aligned}
\mathbf{F^d} &= -C_A \ddot{\mathbf{r}}^n + C_M \dot{\mathbf{V}}^n + C_D \left| \mathbf{V}^n - \ddot{\mathbf{r}}^n \right| \left(\mathbf{V}^n - \ddot{\mathbf{r}}^n \right) \\
&= -C_A \ddot{\mathbf{r}}^n + \overline{\mathbf{F}}^d
\end{aligned}$$

(15)

where C_A is the added mass coefficient per unit length, C_M is the inertial coefficient per unit length per unit normal acceleration and C_D is the drag coefficient per unit length per unit normal velocity. $\mathbf{V}^n$ and $\dot{\mathbf{V}}^n$ are fluid velocity and acceleration normal to the rod centerline respectively. They can be expressed as

$$\mathbf{V}^n = \left(\mathbf{V} - \dot{\mathbf{r}} \right) - \left[\left(\mathbf{V} - \dot{\mathbf{r}} \right) \cdot \mathbf{r'} \right] \mathbf{r'}$$

(16)

$$\dot{\mathbf{V}}^n = \dot{\mathbf{V}} - \left(\mathbf{V} \cdot \dot{\mathbf{r}} \right) \cdot \mathbf{r'}$$

(17)

where $\dot{\mathbf{V}}$ and $\mathbf{V}$ are the total fluid particle's acceleration and velocity at the centerline of the rod without disturbance by the rod. $\ddot{\mathbf{r}}^n$ and $\dot{\mathbf{r}}^n$ are the rod acceleration and velocity normal to its centerline and can be obtained by

$$\dot{\mathbf{r}}^n = \dot{\mathbf{r}} - \left(\dot{\mathbf{r}} \cdot \mathbf{r'} \right) \mathbf{r'}$$

(18)

$$\ddot{\mathbf{r}}^n = \ddot{\mathbf{r}} - \left(\ddot{\mathbf{r}} \cdot \mathbf{r'} \right) \mathbf{r'}$$

(19)

The equation of motion of the rod subjected to its weight, hydrostatic and hydrodynamic forces

in water, combining Equations (13) through (15) with (1) becomes

$$\rho\ddot{\mathbf{r}} + C_a\rho_w\ddot{\mathbf{r}}^n + \left(EI\mathbf{r}''\right)'' - \left(\tilde{\lambda}\mathbf{r}'\right)' = \tilde{\mathbf{w}} + \overline{\mathbf{F}}^d \tag{20}$$

where

$$\tilde{\lambda} = T - EI\kappa^2 \tag{21}$$

$$\tilde{\mathbf{w}} = \mathbf{w} + \mathbf{B} \tag{22}$$

T is the tension in the rod, $\tilde{\mathbf{w}}$ is the effective weight or the wet weight.

The Equation (20) together with the line stretch condition in Equation (12), are the governing equations for the statics or dynamics of the rod in fluid.

In the case of FEAM development, the bending stiffness EI is not included in the governing equations. In many cases, the bending stiffness does not make significant contributions to the platform responses if platform is moored with tensioned lines.

2. Finite Element Model

Since the governing equation is nonlinear, it is difficult to solve the equation by analytically. Therefore, the finite element method is used to transform the differential equations into a series of algebraic equations through an integral statement. For convenience, the governing equations (20) and (21) are written in subscript notation:

$$-\rho\ddot{r}_i - C_a\rho_w\ddot{r}_i^n - \left(EIr_i''\right)'' + \left(\tilde{\lambda}r_i'\right)' + \tilde{w}_i + \overline{F}_i^d = 0 \tag{23}$$

and

$$\frac{1}{2}\left(r_r' \cdot r_r' - 1\right) - \frac{\lambda}{AE} = 0 \tag{24}$$

where the subscripts range from 1 to 2 for the 2 dimensional problem and from 1 to 3 for the 3 dimensional problem. Repeating of the subscripts in the same equation means summation over the subscripts' range.

In the finite element method, the line is discretized into elements with finite length and the algebraic equations are developed in the element level. The unknown variable $r_i(s,t)$, $\lambda(s,t)$ can be approximated as:

$$r_i(s,t) = A_l(s)U_{il}(t) \tag{25}$$

$$\lambda(s,t) = P_m(s)\lambda_m(t) \tag{26}$$

where, $0 \le s \le L$, $A_l(s)$ and $P_m(s)$ are interpolation functions, and $U_{il}(t)$ and $\lambda_m(t)$ are the unknown coefficients. By introducing shape functions for the solution, the weak formulations for applying the finite element method technique are written by multiplying the weight function:

$$\int_0^L \delta r_i \left[-\rho \ddot{r}_i - C_a \rho_w \ddot{r}_i^n - \left(EI r_i'' \right)'' + \left(\tilde{\lambda} r_i' \right)' + \tilde{w}_i + \bar{F}_i^d \right] ds = 0 \tag{27}$$

$$\int_0^L \delta \lambda \left[\frac{1}{2}(r_r' \cdot r_r' - 1) - \frac{\lambda}{AE} \right] ds = 0 \tag{28}$$

The following cubic shape functions for $A_l(s)$ and quadratic shape function for $P_m(s)$ are used for the basis of the relation of $\delta r_i = A_l \delta U_{il}(t)$ and $\delta \lambda = P_m \lambda \delta_m$ such as equation (27) and (28):

$$\begin{aligned}
A_1 &= 1 - 3\xi^2 + 2\xi^3 \\
A_2 &= L\left(\xi - 2\xi^2 + \xi^3 \right) \\
A_3 &= 3\xi^2 - 2\xi^3 \\
A_4 &= L\left(-\xi^2 + \xi^3 \right)
\end{aligned} \tag{29}$$

$$\begin{aligned}
P_1 &= 1 - 3\xi^2 + 2\xi^3 \\
P_2 &= 4\xi(1 - \xi) \\
P_3 &= \xi(2\xi - 1)
\end{aligned} \tag{30}$$

where $\xi = \dfrac{s}{L}$

$$\begin{aligned}
U_{i1} &= r_i(0,t), & U_{i2} &= r_i'(0,t) \\
U_{i3} &= r_i(L,t), & U_{i4} &= r_i'(L,t)
\end{aligned} \tag{31}$$

$$\lambda_1 = \lambda(0,t), \quad \lambda_2 = \lambda(\frac{L}{2},t), \quad \lambda_3 = \lambda(L,t) \tag{32}$$

Thus, the equation (29) and (30) can be written as follows:

$$\int_0^L \delta r_i \left(\rho \ddot{r}_i - C_a \rho_w \ddot{r}_i^n \right) ds = \int_0^L \left(\rho \ddot{r}_i - C_a \rho_w \ddot{r}_i^n \right) A_l \delta U_{il} ds \tag{33}$$

$$\begin{aligned}
\int_0^L \delta r_i \left(EI r_i'' \right)'' ds &= \int_0^L \left(EI r_i'' \right)'' A_l \delta U_{il} ds \\
&= \left[\left(EI r_i'' \right)' A_l \Big|_0^L - EI r_i'' A_l' \Big|_0^L + \int_0^L EI A_l'' r_i'' ds \right] \delta U_{il}
\end{aligned} \tag{34}$$

$$\int_0^L \delta r_i \left(\tilde{\lambda} r_i' \right)' ds = \int_0^L \left(\tilde{\lambda} r_i' \right)' A_i \delta U_{il} ds$$

$$= \left[\left(\tilde{\lambda} r_i' A_i \right) \Big|_0^L + \int_0^L \tilde{\lambda} r_i' A_i' ds \right] \delta U_{il} \tag{35}$$

$$\int_0^L \delta r_i \left[\tilde{w}_i + \overline{F}_i^d \right] ds = \left[\int_0^L \left(\tilde{w}_i + \overline{F}_i^d \right) A_i ds \right] \delta U_{il} \tag{36}$$

$$\int_0^L \delta \lambda \left[\frac{1}{2} (r_r' \cdot r_r' - 1) - \frac{\lambda}{AE} \right] ds = \int_0^L P_m \left[\frac{1}{2} (r_r' \cdot r_r' - 1) - \frac{\lambda}{AE} \right] ds \delta \lambda_m \tag{37}$$

If equations (33) to (36) are assembled and the term of δU_{il} is canceled out on both sides of the above equations, the following equation is obtained:

$$\int_0^L \left\{ A_i \left(\rho \ddot{r}_i - C_a \rho_w \ddot{r}_i^n \right) + EIA_i'' r'' + \tilde{\lambda} r_i' A_i' - A_i \left(\tilde{w}_i + \overline{F}_i^d \right) \right\} ds$$

$$= EIr_i'' A_i' \Big|_0^L + \left[\tilde{\lambda} r_i' + \left(EIr_i'' \right)' \right] A_i \Big|_0^L \tag{38}$$

The same procedures are applied for equation (37) and $\delta \lambda_m$ is removed from both side of the equation (37), and the final form of the equation (37) is:

$$\int_0^L P_m \left[\frac{1}{2} (r_r' \cdot r_r' - 1) - \frac{\lambda}{AE} \right] ds = 0 \tag{39}$$

Thus, the unknown quantities that need to be determined are the position vector and tangent vectors at the two end nodes of the elements and the scalar λ. The λ represents the line tension at the end nodes and the midpoint. By combining equations (19), (25) and (26) with (38) The equation of motion for the element can be written as follows:

$$\left(M_{ijlk} + M_{ijlk}^a \right) \ddot{U}_{jk} + \left(K_{ijlk}^1 + \lambda_n K_{nijlk}^2 \right) U_{jk} - F_{il} = 0 \tag{40}$$

where

$$M_{ijlk} \ddot{U}_{jk} = \int_0^L \rho A_i \ddot{r}_i ds = \int_0^L \rho A_i A_k \delta_{ij} ds \ddot{U}_{jk} \tag{41}$$

$$M_{ijlk}^a \ddot{U}_{jk} = \int_0^L A_i \left(C_A \ddot{r}_i^n \right) ds$$

$$= C_A \left[\int_0^L A_i A_k \delta_{ij} ds - \int_0^L \left(A_i A_k A_s' A_t' \right) U_{it} U_{js} \delta_{ij} ds \right] \ddot{U}_{jk} \tag{42}$$

$$K_{ijlk}^1 U_{jk} = \int_0^L EIA_i'' r_i'' ds = \int_0^L EIA_i'' A_k'' \delta_{ij} ds U_{jk} \tag{43}$$

$$K_{ijlk}^2 U_{jk} = \int_0^L \tilde{\lambda} A_i r_i' ds = \tilde{\lambda}_n \int_0^L P_n A_i' A_k' \delta_{ij} ds U_{jk} \tag{44}$$

$$F_{il} = \int_0^L \left(\tilde{w}_i + \overline{F}_i^d \right) A_i ds \tag{45}$$

and δ_{ij} is the Kronecker Delta function. The resultant forces and moments are not included in this equation, since these forces and moments canceled with the neighboring element during the assembly of the element equation to satisfy the compatibility between two elements. M_{ijlk} in equation (41) represents the mass term and M_{ijlk}^a in equation (42) represents the added mass. In equation (43) and (44), there are two stiffness terms. K_{ijlk}^1 is the material stiffness that comes from the bending stiffness EI, and K_{nijlk}^2 is the stiffness from tension and the curvature of the rod. For the two dimensional problem, i, j = 1, 2 and for the three dimensional problem, i, j = 1, 2, 3 and the subscript l, k, s, t = 1, 2, 3, 4. The equation (39) can be written as:

$$G_m = A_{mil}U_{kl}U_{ki} - B_m - C_{mn}\lambda_n = 0 \tag{46}$$

where

$$A_{mil}U_{jl}U_{jk} = \int_0^L P_m \frac{1}{2}r_r'r_r'ds = \frac{1}{2}\int_0^L P_m A_l'A_k'ds U_{jl}U_{jk} \tag{47}$$

$$B_m = \frac{1}{2}\int_0^L P_m ds \tag{48}$$

$$C_{mn} = \int_0^L P_m \frac{\lambda}{AE}ds = \frac{1}{AE}\int_0^L \lambda_n P_m P_n ds \tag{49}$$

From equations (40) and (46), each element has 12 second-order ordinary differential equations and 3 algebraic equations (3-dimentional problem). All these equations are nonlinear and the force vector, F_{il}, is also a nonlinear function of the unknowns because the wave force varies with the line position. In the next two sections, the numerical treatment for these nonlinear equations is discussed.

2.1 Formulation of Static Problem

In previous section, the equation of motion is derived and expended by finite element method. As mentioned in section 3.3, the numerical treatment of the nonlinear governing equation is discussed in this section and the next section. To analyze the dynamic problem, first the static equilibriums should be obtained. Therefore, in this section, the static problem is discussed. If the inertia term in equation (40) is removed, then the governing equation becomes the static equilibrium equation and it also becomes a nonlinear algebraic equation:

$$R_{il} = 0 \tag{50}$$

$$G_m = 0 \tag{51}$$

where,

$$R_{il} = \left(K^1_{ijlk} + \lambda_n K^2_{nijlk}\right)U_{jk} - F_{il} \tag{52}$$

and F_{il} is a static forcing term from the gravity force, drag force from the steady current and other applied static forces on the line. To solve the nonlinear equations, the Newton-Raphson's iterative method is used. Using the Taylor series expansion, the equation (50) and (51) can be expressed as follow:

$$R_{il}^{(n+1)} = R_{il}^{(n)} + \frac{\partial R_{il}}{\partial U_{jk}}\left(\Delta U_{jk}\right) + \frac{\partial R_{il}}{\partial \lambda_n}\left(\Delta \lambda_n\right) \tag{53}$$

$$G_m^{(n+1)} = G_m^{(n)} + \frac{\partial G_m}{\partial U_{jk}}\left(\Delta U_{jk}\right) + \frac{\partial G_m}{\partial \lambda_n}\left(\Delta \lambda_n\right) \tag{54}$$

where

$$\frac{\partial R_{il}}{\partial U_{jk}} = K^1_{ijlk} + \lambda_n K^2_{nijlk} \tag{55}$$

$$\frac{\partial R_{il}}{\partial \lambda_n} = K^2_{nijlk} \tag{56}$$

$$\frac{\partial G_m}{\partial U_{jk}} = 2A_{mkl}U_{jk} \tag{57}$$

$$\frac{\partial G_m}{\partial \lambda_n} = -C_{mn} \tag{58}$$

and re-arrange the terms,

$$\left(K^1_{ijlk} + \lambda_n K^2_{nijlk}\right)\Delta U_{jk} + \left(K^2_{nijlk}U_{jl}\right)\Delta \lambda_n = -R_{il}^{(n)} \tag{59}$$

$$\left(2A_{mkl}U_{jl}\right)\Delta U_{jk} + \left(-C_{mn}\right)\Delta \lambda_n = -G_m^{(n)} \tag{60}$$

from equation (59) and (60), the equation can be expressed by matrix form as follows:

$$\begin{bmatrix} K^{t0(n)}_{ijlk} & K^{t1(n)}_{i\ln} \\ D^{t0(n)}_{mjk} & D^{t1(n)}_{mn} \end{bmatrix}\begin{Bmatrix} \Delta U_{jk} \\ \Delta \lambda_n \end{Bmatrix} = \begin{Bmatrix} -R_{il}^{(n)} \\ -G_m^{(n)} \end{Bmatrix} \tag{61}$$

where,

$$K^{t0(n)}_{ijlk} = K^1_{ijlk} + \lambda_n^{(n)} K^2_{nijlk} \tag{62}$$

$$K^{t1(n)}_{i\ln} = K^2_{nijlk}U_{jk}^{(n)} = \left(\int_0^L P_n A_l' A_k' ds\right)U_{jk}^{(n)} \tag{63}$$

$$D^{t0(n)}_{mjk} = A_{mkp}U_{jp}^{(n)} = \left(\int_0^L P_m A_k' A_p' ds\right)U_{jp}^{(n)} \tag{64}$$

$$D_{mn}^{t1(n)} = -C_{mn} = -\frac{1}{AE}\int_0^L P_m P_n ds \tag{65}$$

$$R_{il}^{(n)} = \left(K_{ijlk}^1 + \lambda_n K_{nijlk}^2\right)U_{jK}^{(n)} - F_{il} \tag{66}$$

$$G_m^{(n)} = A_{mil}U_{kl}^{(n)}U_{ki}^{(n)} - B_m - C_{mn}\lambda_n^{(n)} = 0 \tag{67}$$

After renumbering, the equation (25) can be written in the form:

$$\mathbf{K}^{(n)}\left(\Delta \mathbf{y}\right) = \mathbf{F}^{(n)} \tag{68}$$

where U_{jk} and λ_n form the vector $\mathbf{y}$

$$\mathbf{y}^T = \begin{bmatrix} U_{11} & U_{12} & U_{21} & U_{22} & U_{31} & U_{32} & \lambda_1 & \lambda_2 & U_{13} & U_{14} & U_{23} & U_{24} & U_{33} & U_{34} & \lambda_3 \end{bmatrix} \tag{69}$$

the force vector is as follows:

$$\mathbf{F}^T = \begin{bmatrix} -R_{11} & -R_{12} & -R_{21} & -R_{22} & -R_{31} & -R_{32} & -G_1 & -G_2 & -R_{13} & -R_{14} & -R_{23} & -R_{24} & -R_{33} & -R_{34} & G_3 \end{bmatrix}$$

(70)

and $\mathbf{K}$ represents stiffness matrix

$$\mathbf{y}^{(n+1)} = \mathbf{y}^{(n)} + \Delta \mathbf{y} \tag{71}$$

In every iterative step, the stiffness and the force vector are recalculated to solve for $\Delta \mathbf{y}$. Because one element has 15 algebraic equation, the band width of the stiffness matrix is 15, and total number of equations for one rod is $(N+1)\times 8 - 1$, where N is number of elements in a rod. From right hand side of the equation (38), the force vector can be written as:

$$F^r = \begin{bmatrix} -\left[\lambda r_1' + (Br_1'')'\right]A_l\Big|_{s=0} \\[4pt] \left[EIr_1''\right]A_l'\Big|_{s=0} \\[4pt] -\left[\lambda r_2' + (Br_2'')'\right]A_l\Big|_{s=0} \\[4pt] \left[EIr_2''\right]A_2'\Big|_{s=0} \\[4pt] -\left[\lambda r_3' + (Br_3'')'\right]A_l\Big|_{s=0} \\[4pt] \left[EIr_3''\right]A_3'\Big|_{s=0} \\[4pt] 0 \\[2pt] 0 \\[4pt] \left[\lambda r_1' + (Br_1'')'\right]A_l\Big|_{s=L} \\[4pt] -\left[EIr_1''\right]A_l'\Big|_{s=L} \\[4pt] \left[\lambda r_2' + (Br_2'')'\right]A_l\Big|_{s=L} \\[4pt] -\left[EIr_2''\right]A_2'\Big|_{s=L} \\[4pt] \left[\lambda r_3' + (Br_3'')'\right]A_l\Big|_{s=L} \\[4pt] \left[EIr_3''\right]A_l'\Big|_{s=L} \\[2pt] 0 \end{bmatrix} = \begin{bmatrix} -N_1^{[1]} \\ -L_1^{[1]} \\ -N_2^{[1]} \\ -L_2^{[1]} \\ -N_3^{[1]} \\ -L_3^{[1]} \\ 0 \\ 0 \\ -N_1^{[2]} \\ -L_1^{[2]} \\ -N_2^{[2]} \\ -L_2^{[2]} \\ -N_3^{[2]} \\ -L_3^{[2]} \\ 0 \end{bmatrix} \qquad (72)$$

where the superscript [1] represents the first end of the element (s = 0) and [2] represents the second end (s = L). $N = \{N_1, N_2, N_3\}^T$ represents the nodal resultant force and $L = \{L_1, L_2, L_3\}^T$ represents the nodal resultant moment $M(M = L \times r')$. Therefore, after solving the variables U and λ (at iteration n+1), the resultant force at the end nodes of an element can be obtained from force vector $\mathbf{F^r}$

$$\mathbf{F}^r = -\mathbf{F}^{(n+1)} \qquad (73)$$

2.2 Formulation for Dynamic Problem – Time Domain Integration

The dynamic equation of motion (40), and the stretch condition (46) can be rearrange as follows:

$$\widehat{M}_{ijlk}\ddot{U}_{jk} = -\left(K^1_{ijlk} + \lambda_n K^2_{nijlk}\right)U_{jk} + F_{il} = \widehat{F}_{il} \qquad (74)$$

$$G_m = A_{mil}U_{kl}U_{ki} - B_m - C_{mn}\lambda_n = 0 \qquad (75)$$

where,

$$\widehat{M}_{ijlk} = M_{ijlk} + M^a_{ijlk} \qquad (76)$$

$$\widehat{F}_{il} = -F_{il}^1 - F_{il}^2 + F_{il} \tag{77}$$

$$F_{il}^1 = K_{ijlk}^1 U_{jk} \tag{78}$$

$$F_{il}^2 = \lambda_n K_{nijlk}^2 U_{jk} \tag{79}$$

The equation (76) is a second order differential equation and (75) is algebraic equation with no time derivatives of the variables. To establish the time integration numerical scheme, equation (76) is split into two first order differential equations:

$$\widehat{M}_{ijlk} \dot{V}_{jk} = \widehat{F}_{il} \tag{80}$$

$$\dot{U}_{jk} = V_{jk} \tag{81}$$

Integrating the above two equations from time $t^{(n)}$ (at n^{th} time step) to $t^{(n+1)}$ (at $n+1^{th}$ time step) the equation can be written as:

$$\int_{t(n)}^{t(n+1)} \widehat{M}_{ijlk} \dot{V}_{jk} dt = \int_{t(n)}^{t(n+1)} \widehat{F}_{il} dt \tag{82}$$

$$\int_{t(n)}^{t(n+1)} \dot{U}_{jk} dt = \int_{t(n)}^{t(n+1)} V_{jk} dt \tag{83}$$

Because $\widehat{M}_{ijlk}$ includes the added mass, the mass term is not constant, and it varies with line position, which means it is a function of time. By approximating the time varying $\widehat{M}_{ijlk}$ in time interval $\Delta t(t^{(n+1)} - t^{(n)})$ to be a constant $\widehat{M}_{ijlk}^{(n+\frac{1}{2})}$, which is the mass at $t^{(n)} + \dfrac{\Delta t}{2}$, then the integration in equation (82) can be simplified as follows with second order accuracy as:

$$\widehat{M}_{ijlk}^{(n+\frac{1}{2})} \dot{V}_{jk}^{(n+1)} + \widehat{M}_{ijlk}^{(n+\frac{1}{2})} \dot{V}_{jk}^{(n)} = \int_{t(n)}^{t(n+1)} \widehat{F}_{il} dt \tag{84}$$

The $V_{jk}^{(n+1)}$ of the equation (83) can be obtained as follows using trapezoidal methods:

$$U_{jk}^{(n+1)} = U_{jk}^{(n)} + \frac{\Delta t}{2} \left(V_{jk}^{(n+1)} + V_{jk}^{(n)} \right) \tag{85}$$

Re-arranging equation (84) and (85), the equation becomes:

$$\frac{4}{\Delta t^2} \widehat{M}_{ijlk}^{(n+\frac{1}{2})} \Delta U_{jk} = \frac{4}{\Delta t^2} \widehat{M}_{ijlk}^{(n+\frac{1}{2})} V_{jk}^{(n)} + \frac{2}{\Delta t} \int_{t(n)}^{t(n+1)} \widehat{F}_{il} dt \tag{86}$$

$$V_{jk}^{(n+1)} = \frac{2}{\Delta t} \left(\Delta U_{jk} \right) - V_{jk}^{(n)} \tag{87}$$

where

$$\Delta U_{jk}^{(n+1)} = U_{jk}^{(n+1)} - U_{jk}^{(n)} = \frac{\Delta t}{2} \left(V_{jk}^{(n+1)} + V_{jk}^{(n)} \right) \tag{88}$$

and the integral term in equation (84) can be written as:

$$\int_{t(n)}^{t(n+1)} \widehat{F}_{il} dt = -\int_{t(n)}^{t(n+1)} F_{il}^1 dt - \int_{t(n)}^{t(n+1)} F_{il}^2 dt + \int_{t(n)}^{t(n+1)} F_{il} dt \tag{89}$$

For the first and second terms at the right hand side, applying trapezoidal rules, then

$$\begin{aligned}
\int_{t(n)}^{t(n+1)} F_{il}^1 dt &= \frac{\Delta t}{2}\left(F_{il}^{1(n+1)} + F_{il}^{1(n)}\right)\\
&= \frac{\Delta t}{2}\left[K_{ijlk}^1 \Delta U_{jk} + 2K_{ijlk}^1 U_{jk}^{(n)}\right]
\end{aligned} \tag{90}$$

$$\begin{aligned}
\int_{t(n)}^{t(n+1)} F_{il}^2 dt &= \frac{\Delta t}{2}\left(F_{il}^{2(n+1)} + F_{il}^{2(n)}\right)\\
&= \frac{\Delta t}{2}\left[\lambda_n^{(n+1)} K_{nijlk}^2 U_{jk}^{(n+1)} + \lambda_n^{(n)} K_{nijlk}^2 U_{jk}^{(n)}\right]\\
&\approx \frac{\Delta t}{2}\left[\lambda_n^{(n+\frac{1}{2})} K_{nijlk}^2 U_{jk}^{(n+1)} + \lambda_n^{(n+\frac{1}{2})} K_{nijlk}^2 U_{jk}^{(n)}\right]\\
&= \frac{\Delta t}{2}\left[2\lambda_n^{(n+\frac{1}{2})} K_{nijlk}^2 U_{jk}^{(n)} + 2K_{nijlk}^2 U_{jk}^{(n)} \Delta\lambda_n + \lambda_n^{(n-\frac{1}{2})} K_{nijlk}^2 \Delta U_{jk}\right]
\end{aligned} \tag{91}$$

where $\Delta\lambda_n = \lambda_n^{(n+\frac{1}{2})} - \lambda_n^{(n-\frac{1}{2})}$. The third term in equation (89) includes the applied force F_{il} which is from gravity and hydrodynamic forces. The gravity force is independent of time, but the hydrodynamic force form Morison equation is unknown at time step (n+1) since the force is function of the unknown rod position and velocity. Therefore, the Adams-Bashforth explicit scheme is used for the integration:

$$\int_{t(n)}^{t(n+1)} F_{il}^2 dt = \begin{cases} \Delta t F_{il}^{(0)} & \text{for step1} \\ \dfrac{\Delta t}{2}\left(3F_{il}^{(n)} + F_{il}^{(n-1)}\right) & \text{for other step} \end{cases} \tag{92}$$

Using the above equations, the time integration equation (84) can be obtained as follows:

$$\begin{aligned}
&\left[\frac{4}{\Delta t^2}\widehat{M}_{ijlk}^{(n+\frac{1}{2})} + K_{ijlk}^1 + \lambda_n^{(n-\frac{1}{2})} K_{nijlk}^2\right]\Delta U_{jk} + 2K_{nijlk}^2 U_{jk}^{(n)} \Delta\lambda_n\\
&= \frac{4}{\Delta t^2}\widehat{M}_{ijlk}^{(n+\frac{1}{2})} V_{jk}^{(n)} + \left(3F_{il}^{(n)} - F_{il}^{(n-1)}\right) - 2K_{ijlk}^1 U_{jk}^{(n)} - 2\lambda_n^{(n+\frac{1}{2})} K_{nijlk}^2 U_{jk}^{(n)}
\end{aligned} \tag{93}$$

Using Adams-Bashforth method can approximate the time varying mass:

$$\widehat{M}_{ijlk}^{(n+\frac{1}{2})} = \frac{1}{2}\left(3\widehat{M}_{ijlk}^{(n)} - \widehat{M}_{ijlk}^{(n-1)}\right) \tag{94}$$

For the stretch condition (equation (75)), the time marching can be obtained by Taylor expansion

$$0 = 2G_m^{(n+1)} \approx 2G_m^{(n)} + 2\frac{\partial G_m}{\partial U_{jk}}\Delta U_{jk} + 2\frac{\partial G_m}{\partial \lambda_n}\Delta \lambda_n$$

$$= 2G_m^{(n)} + 2K_{mijlk}^2 U_{il}\Delta U_{jk} - 2C_{mn}\Delta \lambda_n \tag{95}$$

$$= 2G_m^{(n)} + \widehat{D}_{mjk}^{t0(n)}\Delta U_{jk} - 2\widehat{D}_{mn}^{t1(n)}\Delta \lambda_n$$

Using equation (94) and (95), the equation of motion and the stretch condition can be re-written as follows:

$$\widehat{K}_{ijlk}^{t0(n)}\Delta U_{jk} + \widehat{K}_{lin}^{t1(n)}\Delta \lambda_n = -\widehat{R}_{il} \tag{96}$$

$$\widehat{D}_{mjk}^{t0(n)}\Delta U_{jk} + \widehat{D}_{mn}^{t1(n)}\Delta \lambda_n = -\widehat{G}_m \tag{97}$$

where

$$\widehat{K}_{ijlk}^{t0(n)} = \frac{2}{\Delta t^2}\left(3\widehat{M}_{ijlk}^{(n)} - \widehat{M}_{ijlk}^{(n-1)}\right) + K_{ijlk}^1 + \lambda_n^{\left(n-\frac{1}{2}\right)}K_{nijlk}^2 \tag{98}$$

$$\widehat{K}_{lin}^{t1(n)} = 2K_{nijlk}^2 U_{jk}^{(n)} \tag{99}$$

$$\widehat{D}_{mjk}^{t0(n)} = 2K_{nijlk}^2 U_{jk}^{(n)} \tag{100}$$

$$\widehat{D}_{mn}^{t1(n)} = -2C_{mn} = 2D_{mn}^{t1(n)} \tag{101}$$

$$\widehat{R}_{il} = \frac{2}{\Delta t^2}\left(3\widehat{M}_{ijlk}^{(n)} - \widehat{M}_{ijlk}^{(n-1)}\right) + \left(3F_{il}^{(n)} - F_{il}^{(n-1)}\right)$$

$$- 2K_{ijlk}^1 U_{jk}^{(n)} - 2\lambda_n^{\left(n+\frac{1}{2}\right)}K_{nijlk}^2 U_{jk}^{(n)} \tag{102}$$

$$\widehat{G}_m^{(n)} = 2G_m^{(n)} \tag{103}$$

The resultant forms of the equation (96) and (97) are similar to the static problem. The equation of motion in matrix form can be written as follows:

$$\widehat{\mathbf{K}}^{(n)}\left(\Delta \mathbf{y}\right) = \widehat{\mathbf{F}}^{(n)} \qquad \text{at time step n} \tag{104}$$

$$\mathbf{F}^r = -\widehat{\mathbf{F}}^{(n+1)} \tag{105}$$

Using Adams-Moulton with Adams-Bashforth scheme, the numerical methods in this study, mixed implicit and explicit scheme is used to avoid iterative methods in time domain problem.

2.3 Modeling of the Seafloor

For the catenary mooring system, a portion of a mooring line near the anchor usually lies on the seabed. The interaction between steel catenary riser and the seafloor is also very important in the riser design. Due to this reason, the interaction between mooring line (or riser) and seafloor is modeled. In the numerical modeling, the horizontal friction between line and seafloor are neglected. However, in vertical direction, the seafloor is modeled as elastic

foundation, and the dynamic bottom boundary conditions are shown in following equations:

$$f_1 = 0, \quad f_2 = 0, \quad f_3 = \begin{cases} c(r_3 - D)^2 & \text{for } r_3 - D < 0 \\ 0 & \text{for } r_3 - D \geq 0 \end{cases} \tag{106}$$

where D represents the water depth or vertical distance between the seafloor and the origin of the coordinate, and r_3 is the z-component of the line position vector. Include seafloor interaction, the equation of motion is re-written as follows:

$$\left(M_{ijlk} + M_{ijlk}^a \right) \ddot{U}_{jk} + \left(K_{ijlk}^1 + \lambda_n K_{nijlk}^2 \right) U_{jk} = F_{il} + F_{il}^f \tag{107}$$

where

$$F_{il}^f = \begin{cases} \int_0^L A_l \delta_{i3} c(r_3 - D)^2 & \text{for } r_3 - D < 0 \\ 0 & \text{for } r_3 - D \geq 0 \end{cases}$$

$$= \begin{cases} \int_0^L A_l \delta_{i3} c(\delta_{i3} A_k U_{jk} - D)^2 & \text{for } r_3 - D < 0 \\ 0 & \text{for } r_3 - D \geq 0 \end{cases} \tag{108}$$

and,

$$\delta_{i3} = \begin{cases} 1 & \text{for i=3} \\ 0 & \text{otherwise} \end{cases} \quad \text{(Kronecker Delta)} \tag{109}$$

In the static analysis, the stiffness matrix is modified as follows:

$$K_{ijlk}^3 = \frac{\partial F_{il}^f}{\partial U_{jk}}$$

$$= \begin{cases} \int_0^L 2 A_l \delta_{i3} c \delta_{j3} A_k (\delta_{m3} A_n U_{mn}^{(n)} - D)^2 & \text{for } r_3 - D < 0 \\ 0 & \text{for } r_3 - D \geq 0 \end{cases} \tag{110}$$

The additional stiffness K_{ijlk}^3 from seafloor is added to K_{ijlk}^{t0}. In the time domain analysis using the trapezoidal rule, the stiffness matrix modified as follows:

$$\int_{t(n)}^{t(n+1)} F_{il}^f dt = \frac{\Delta t}{2} \left(F_{il}^{f(n+1)} + F_{il}^{f(n)} \right)$$

$$= \frac{\Delta t}{2} \left[K_{ijlk}^3 \Delta U_{jk} + 2 F_{il}^{f(n)} \right] \tag{111}$$

The equation of motion includes seafloor effects finally written as follows:

$$\left[\frac{4}{\Delta t^2} \widehat{M}_{ijlk}^{(n+\frac{1}{2})} + K_{ijlk}^1 + \lambda_n^{(n-\frac{1}{2})} K_{nijlk}^2 \right] \Delta U_{jk} + 2K_{nijlk}^2 U_{jk}^{(n)} \Delta \lambda_n$$

$$= \frac{4}{\Delta t^2} \widehat{M}_{ijlk}^{(n+\frac{1}{2})} V_{jk}^{(n)} + \left(3F_{il}^{(n)} - F_{il}^{(n-1)} + 2F_{il}^{f(n)} \right) - 2K_{ijlk}^1 U_{jk}^{(n)} - 2\lambda_n^{(n+\frac{1}{2})} K_{nijlk}^2 U_{jk}^{(n)}$$

(112)

3. Input Data

The FEAM mooring module input file contains the information about mooring system (element definition, material property, platform-mooring coupling, and mooring line boundary conditions)

The input data are dimensional and standard unit systems are used (meters, kg, Newton and second for SI system).

In the FEAM input file, the x and y axis define a horizontal plane and z axis is positive upward. The origins of the global coordinate systems are located on the mean water surface with the corresponding axis parallel to each other. All the information related to the mooring system is defined with respect to the global coordinate system. In the following sections, all the input and output data are given in global coordinate except those specified otherwise.

The input data can be divided into two groups. The first group of data contains general information needed in the program and is listed as follows

DT: Communication interval for controllers

NumLines: The total number of mooring lines

NumElem: The total number of elements per line. All elements are equal in length.

Gravity: Gravitational acceleration

WtrDens: Water density

MaxIter: The maximum number of iterations for finding static equilibrium position of lines. In most cases, 100 is enough.

Eps: Static iteration tolerance.

The second group of data contains all the properties of mooring lines including material

properties, geometry, boundary conditions. This group of data should be prepared for every line. In other words, one should repeat this group of input data for NumLines times, where NumLines is the total number of lines as defined in group one.

LEAStiff: The axial stiffness (Young's modulus cross sectional area of the line) in [N]

LMassDen: The mass per unit length of the element in [kg/m]

LDMassDen: The displaced mass per unit length if the element is in water (LDMassDen =0 if the element is in air) in [kg/m]

LineCI: The coefficient of inertial force in [kg/m], i.e., the inertia force per unit length at unit acceleration.

LineCD: The coefficient of drag force in [kg/m^2], i.e., the drag force per unit length at unit relative velocity squared.

LUnstrLen: The unstretched line length in [m]

BottmStiff: The stiffness coefficient of the foundation. In the program, the elastic foundation is modeled as a continuous quadratic spring foundation to support the lines, i.e. the relation between the vertical support force *F* and the vertical deformation *dz* is *F=BottmStiff* $\times$ *dz^2* in [N/m^2]

LRadAnch: The anchor point radius in [m]

LAngAnch: The anchor point angle in [deg]

LDpthAnch: The anchor point depth in [m]

LRadFair: The fairlead point radius in [m]

LAngFair: The fairlead point angle in [deg]

LDrftFair: The fairlead point draft in [m]

Tension: The pretension at the fairlead point. This input affects axial deformation of the element in the analysis. For example, in a TLP analysis, if the stretch of the tether caused by the net buoyancy force is already included in the initial element length (LUnstrLen), one needs to set the 'Tension' as the actual static pretension so that any axial deformation in the calculation is caused only by dynamic tension

XSpringStiff, YSpringStiff, ZSpringStiff: The linear spring stiffness between mooring line top and platform fairlead along x, y and z direction respectively in [N/m]. The user can vary the stiffness to simulate different types of connections. It is recommended that the values of stiffness should be about 100~1,000 times higher than the axial (stretch) stiffness (LEAStiff)

of the lines.

OutList: Currently, FEAM can produce the tensions at fairlead and anchor position. The output channels are listed below. The maximum number of lines are not limited in the computation, but the maximum number of output lines are set to 10.

Table 1. FEAM output channels

Name	Description
FairT1	Fairlead tension of line #1 [kN]
FairT2	Fairlead tension of line #2 [kN]
…	…
FairT10	Fairlead tension of line #10 [kN]
AnchT1	Anchor tension of line #1 [kN]
AnchT2	Anchor tension of line #2 [kN]
…	…
AnchT10	Anchor tension of line #10 [kN]

4. Subroutines and internal variables

The subroutines inside the FEAM module are explained in this section.

FEAM_Init: In this subroutine, the input file data are loaded and initial line stiffness matrix is made. Then it calls 'FEAM_Solve' to find the static equilibrium of line position.

FEAM_UpdateStates: This subroutine updates the states variables by calling 'FEAM_Solve'. Since p%DYN = true in this subroutine, 'FEAM_Solve' compute the dynamic equation of motion of lines. The current fairlead positions in global coordinate system are fed into 'FEAM_Solve'. In addition, this subroutine saves the current position of fairlead into 'OtherState%FAST_FPA' in order to use numerical integration of the next time step.

FEAM_CalcOutput: This subroutine calculates outputs. The outputs in this subroutine are listed below.

Table 2. Output variables in FEAM_CalcOutput

Name	Description	Index
OtherState%FAIR_T(LEG)	Fairlead tension [N]	LEG : Line number
OtherState%ANCH_T(LEG)	Anchor tension [N]	
OtherState%FAIR_ANG(LEG,I)	Unit tangent vector component of fairlead angle	LEG : Line number I : Direction (x,y,z)
OtherState%ANCH_ANG(LEG,I)	Unit tangent vector component of anchor angle	
OtherState%Line_Coordinate(LEG,I,J)	Line element coordinate	LEG : Line number I : Node number J : Direction (x,y,z)
OtherState%Line_Tangent(LEG,I,J)	Line element tangent vector at nodes	
OtherState%F_Lines(LEG,J)	Mooring restoring force [N]	

FEAM_Solve: If DYN = false, this subroutine calculate the initial static configuration of lines. Otherwise, it solves the dynamic equation of motion of lines.

Element: This subroutine fills out the mass, stiffness and force matrix of one line element. The forces acting on the element include gravity, seabed quadratic spring and hydrodynamic force from Morison equation. The hydrodynamic force on one line element of length 'p%Elength' should be inserted into 'OtherState%FORCE'. The details of key variables are tabulated below.

Table 3. Key variables in 'Element' subroutine

Name	Description	Remark
OtherState%U(1,1)	X Coordinate of 1st end	
OtherState%U(2,1)	Y Coordinate of 1st end	
OtherState%U(3,1)	Z Coordinate of 1st end	
OtherState%U(1,3)	X Coordinate of 2nd end	
OtherState%U(2,3)	Y Coordinate of 2nd end	
OtherState%U(3,3)	Z Coordinate of 2nd end	
OtherState%U(1,2)	X component of direction cosine of 1st end	
OtherState%U(2,2)	Y component of direction cosine of 1st end	
OtherState%U(3,2)	Z component of direction cosine of 1st end	
OtherState%U(1,4)	X component of direction cosine of 2nd end	
OtherState%U(2,4)	Y component of direction cosine of 2nd end	
OtherState%U(3,4)	Z component of direction cosine of 2nd end	

All the above coordinates and forces should be written with respect to the global coordinate system at current simulation time 't'. The 'u%HydroForceLineMesh' variable contains the information of the line coordinate inside 'position'

Couple: This subroutine calculates the spring connector force and stiffness coefficients between line ends and platform. The right hand side 'RHSR' should be calculated based on both the previous fairlead position and the current fairlead position for numerical integrations. This is why 'FEAM_Solve' always calls 'Couple' subroutine twice.

Solve: This is a generic subroutine for solving systems of equations using Gauss elimination.

5. Example

In this section, OC3-Hywind spar mooring lines are modeled using FEAMooing module.

```
--------------------- FAST MOORING FILE -------------------------------------
NREL 5.0 MW offshore baseline floating platform input properties for the OC3-Hywind spar-buoy.
--------------------- SIMULATION CONTROL -------------------------------------
False           Echo               - Echo input data to <RootName>.ech (flag)
       0.0125   DT                 - Communication interval for controllers (s)
       3        NumLines           - Number of lines
       20       NumElem            - Total number of elements per line
       9.81     Gravity            - Gravitational acceleration (m/s^2)
   1025.0       WtrDens            - Water density (kg/m^3)
       100      MaxIter            - Maximum number of static iterations
       1e-4     Eps                - Static iteration tolerance
--------------------- MOORING LINES 1 ----------------------------------------
   384.243E6    LEAStiff           - Axial stiffness
       77.7     LMassDen           - Mass per unit length of the element
       6.47     LDMassDen          - Displaced mass per unit length of the element
       6.47     LineCI             - The inertia force per unit length / unit accel.
       46.13    LineCD             - The draf force per unit length / unit relative vel.
       902.2    LUnstrLen          - Unstretched length
       1.0E4    BottmStiff         - Seabed stiffness
   855.574      LRadAnch
       0.0      LAngAnch
       320.0    LDpthAnch
       4.7      LRadFair
       0.0      LAngFair
       70.0     LDrftFair
       9.7E5    Tension            - Initial top tension
```

1.0E10	XSpringStiff	- The linear spring stiffness in x-direction between mooring & platform
1.0E10	YSpringStiff	- The linear spring stiffness in y-direction between mooring & platform
1.0E10	ZSpringStiff	- The linear spring stiffness in z-direction between mooring & platform

---------------------- MOORING LINES 2 ---

384.243E6	LEAStiff	- Axial stiffness
77.7	LMassDen	- Mass per unit length of the element
6.47	LDMassDen	- Displaced mass per unit length of the element
6.47	LineCI	- The inertia force per unit length / unit accel.
46.13	LineCD	- The draf force per unit length / unit relative vel.
902.2	LUnstrLen	- Unstretched length
1.0E4	BottmStiff	- Seabed stiffness
855.574	LRadAnch	
120.0	LAngAnch	
320.0	LDpthAnch	
4.7	LRadFair	
120.0	LAngFair	
70.0	LDrftFair	
9.7E5	Tension	- Initial top tension
1.0E10	XSpringStiff	- The linear spring stiffness in x-direction between mooring & platform
1.0E10	YSpringStiff	- The linear spring stiffness in y-direction between mooring & platform
1.0E10	ZSpringStiff	- The linear spring stiffness in z-direction between mooring & platform

---------------------- MOORING LINES 3 ---

384.243E6	LEAStiff	- Axial stiffness
77.7	LMassDen	- Mass per unit length of the element
6.47	LDMassDen	- Displaced mass per unit length of the element
6.47	LineCI	- The inertia force per unit length / unit accel.
46.13	LineCD	- The draf force per unit length / unit relative vel.
902.2	LUnstrLen	- Unstretched length
1.0E4	BottmStiff	- Seabed stiffness
855.574	LRadAnch	
240.0	LAngAnch	
320.0	LDpthAnch	
4.7	LRadFair	
240.0	LAngFair	
70.0	LDrftFair	
9.7E5	Tension	- Initial top tension
1.0E10	XSpringStiff	- The linear spring stiffness in x-direction between mooring & platform
1.0E10	YSpringStiff	- The linear spring stiffness in y-direction between mooring & platform
1.0E10	ZSpringStiff	- The linear spring stiffness in z-direction between mooring & platform

---------------------- OUTPUT ---

True	SumPrint	- Print summary data to <RootName>.sum (flag) (currently unused)
1	OutFile	
True	TabDelim	
"ES10.3E2"	OutFmt	
5	TStart	
	OutList	

END of input file (the word "END" must appear in the first 3 columns of this last OutList line)

In this example, three mooring lines are modeled. The angle between each line is 120 degrees, and the radius of anchor position is 855.574m. The initial pretensions of the mooring lines are set to 9.7e5N per line and its direction is tangent to the end of the line element. The pretensions are used to find the initial equilibrium position of floating platform. If this pretension is too small, the initial equilibrium position will be greater than MWL for example. The linear spring stiffness between mooring line end and fairlead is 1.0e10 N/m for all x, y and z direction.
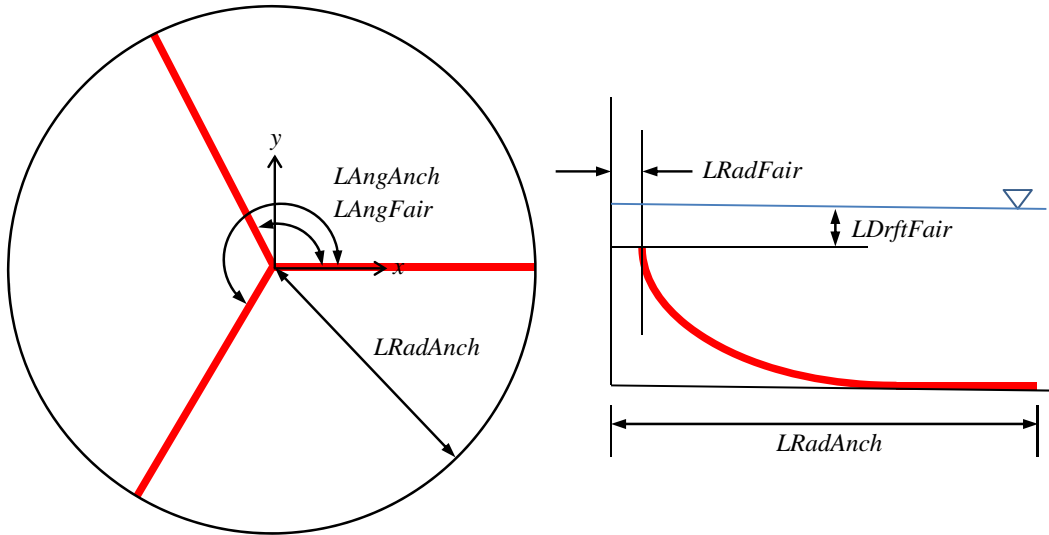
Figure 2. OC3-Hywind mooring lines

During the dynamic simulation, the hydrodynamic loadings on the line elements are calculated at each time step. In the FEAM module, the wave kinematics at line nodes come from the initial line position not from the current line position. However, this does not make significant error because the wave kinematics at different position make a negligible effect on the mooring line dynamics.

6. Verification test

To verify the FEAM module in new FAST framework, free-decay test of OC3-Hywind spar platform was conducted and compared with the result from the FAST-CHARM3D simulation. The FAST-CHARM3D program was developed by TAMU based on the external coupling of the two programs, FASTv7 and CHARM3D. It is a totally independently developed program

and has been verified extensively in various case studies. The FASTv8+FEAM is the newly developed program in this project for equivalent capability while conforming to the new frame of FASTv8 modular structure.

To eliminate the inconsistent conditions between FAST-CHARM3D and FAST-FEAM, below constraints are applied

- Aerodynamics is not included. (CompAero = False)
- WaveMod is set to 0, which means the test is conducted in a still water condition.
- Hull viscous drag (Cd = 0.6) is not included.
- Rotor does not rotate.

Initial offset position of the surge is set to 4m and released. The surge displacement and mooring line tensions are plotted and compared in this section.
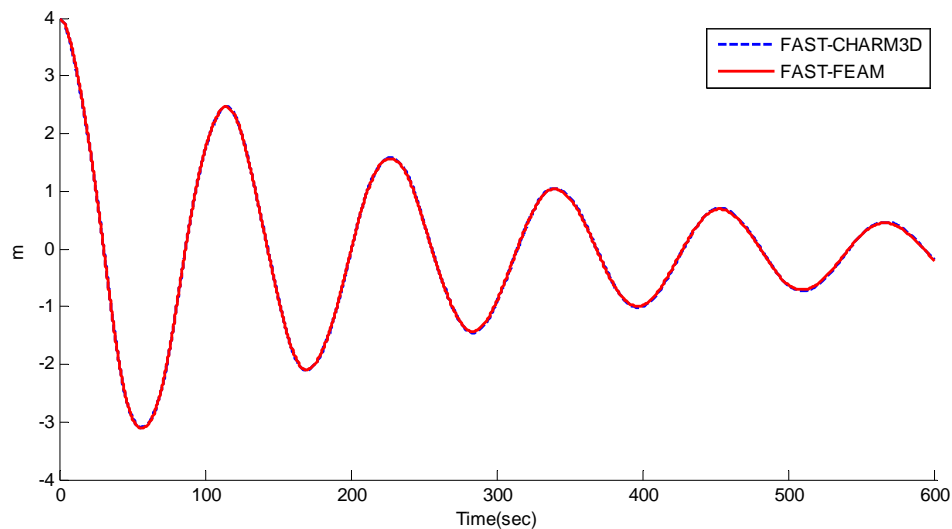
Figure 3. Surge free decay test

As can be seen in Fig. 3, the time series of the surge displacement shows very good agreement between FAST-CHARM3D and FAST-FEAM. Minor differences which can be seen in the figure come from the slightly different hydrodynamic module and different platform initial offset. (FAST-CHARM3D applies force or moment to move the platform to the initial position of the free decay test. For this reason, FAST-CHARM3D needs to apply surge force, heave force and pitch moment for fair comparison with FAST-FEAM)
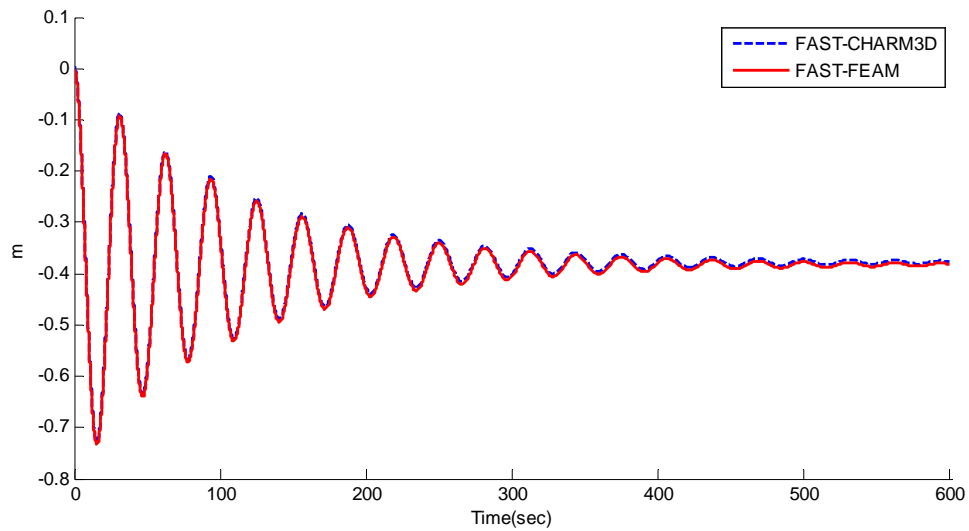
Figure 4. Heave response during surge free decay test
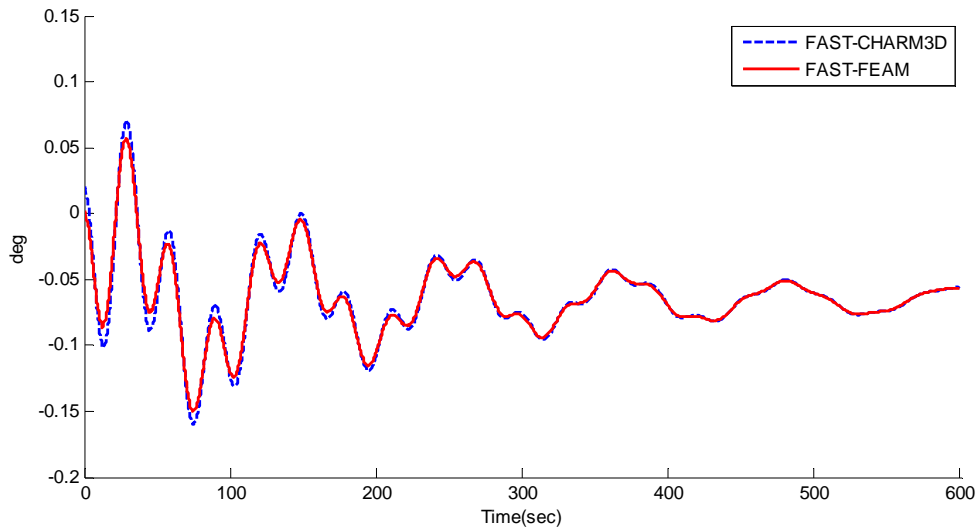
Figure 5. Pitch response during surge free decay test

Figs. 4~5 show the platform heave and pitch responses during the surge free decay test. Those responses also show very good agreement between FAST-CHARM3D and FAST-FEAM. Minor differences in the transient stage of the pitch are due to the slight different initial position of the pitch. The excellent agreement of the natural periods also confirms that the mooring stiffness is modeled correctly.
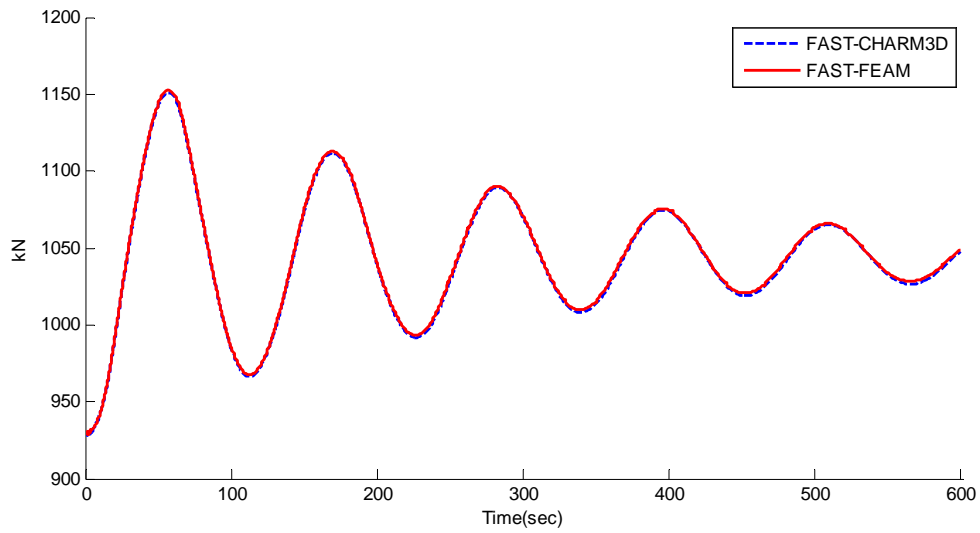
Figure 6. Top tension of the mooring line #1

Similarly, the mooring line top tensions are also compared in Figs. 6~8. The top tensions also show good agreement. The minor differences come from the small different initial conditions between FAST-CHARM3D and FAST-FEAM and the difference ratio is less than 0.4%.
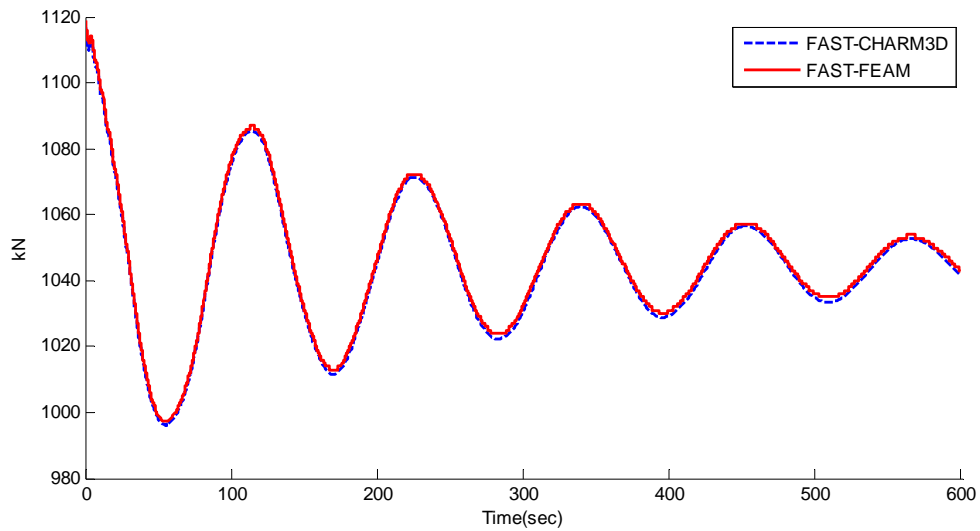
Figure 7. Top tension of the mooring line #2
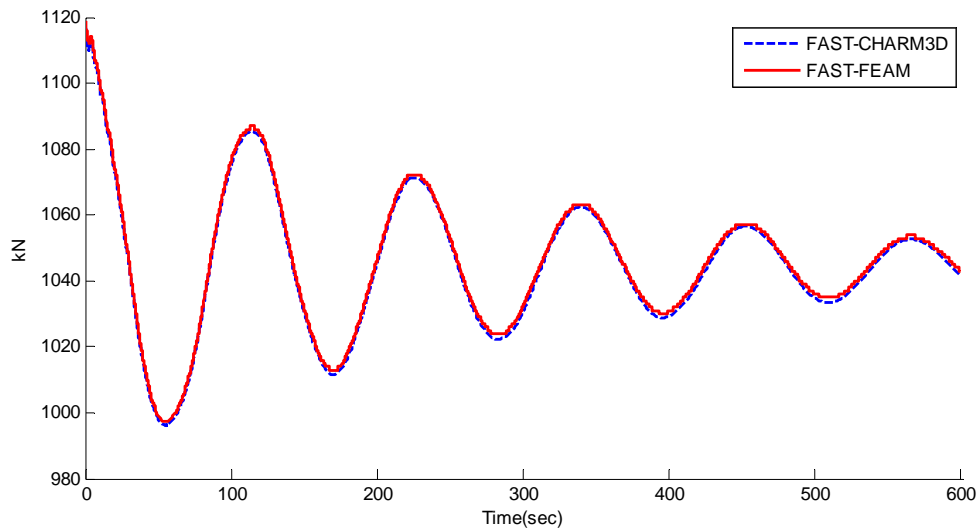
Figure 8. Top tension of the mooring line #3

In the FEAM module, the mooring-line dynamics calculated by Morison's equation are included with proper inertial coefficient (CI) and drag coefficient (CD). The current mooring line module inside the FAST (MAP module or 'Catenary' subroutine) cannot consider the effect of the hydrodynamic loading on the lines. To see the effect of the hydrodynamic loadings on the lines, two cases (with CD and CI, without CD and CI) are simulated using newly developed FEAM module. The difference can be considered as mooring damping.
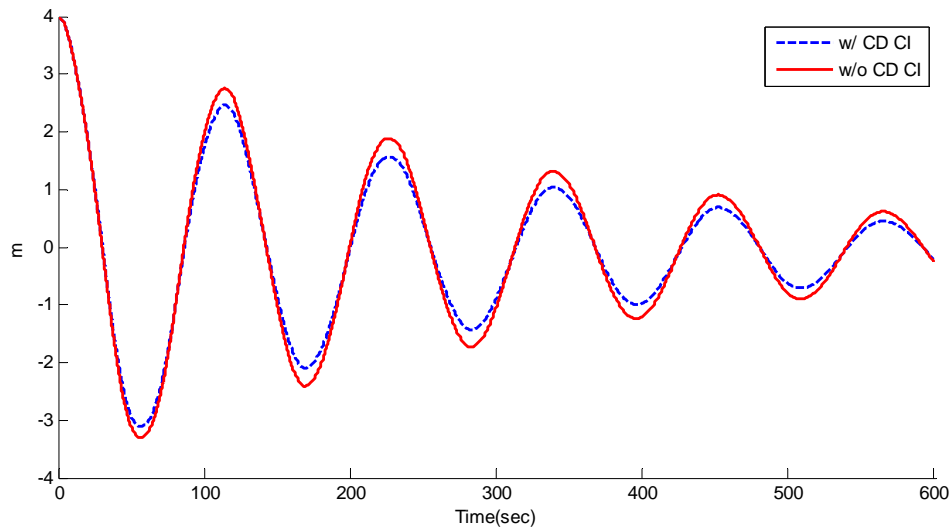
Figure 9. The effect of the mooring dynamics on the platform surge

As can be seen in Fig.9, the natural frequency of the platform does not change, but the decaying ratio changes due to the damping from the mooring line drag. In deep water, this effect could be significant, so should be included in the computation.

Other than the free decay test, regular wave test was also conducted. All the conditions are same as the free decay test without any initial platform offsets. The incident-wave period is set to 10s, and the wave height is 6m.
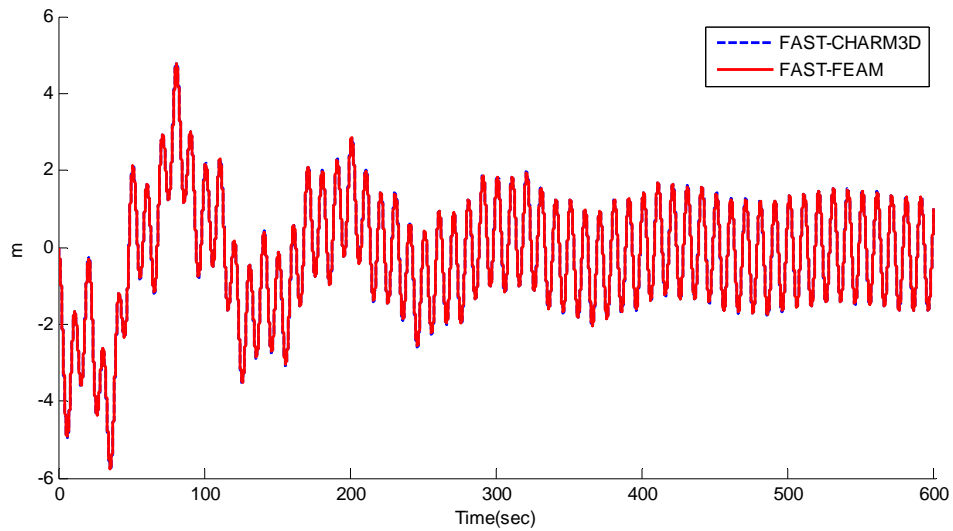

Figure 10. Platform surge with regular wave
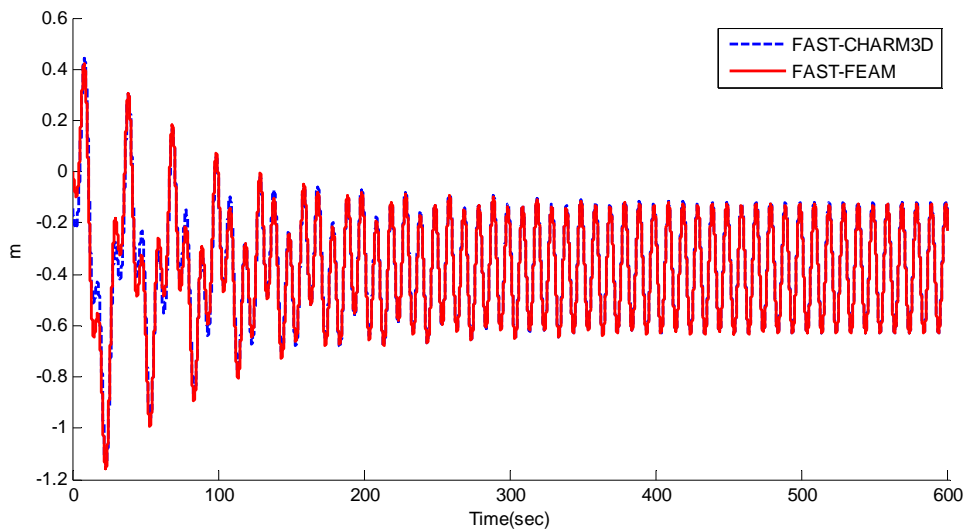
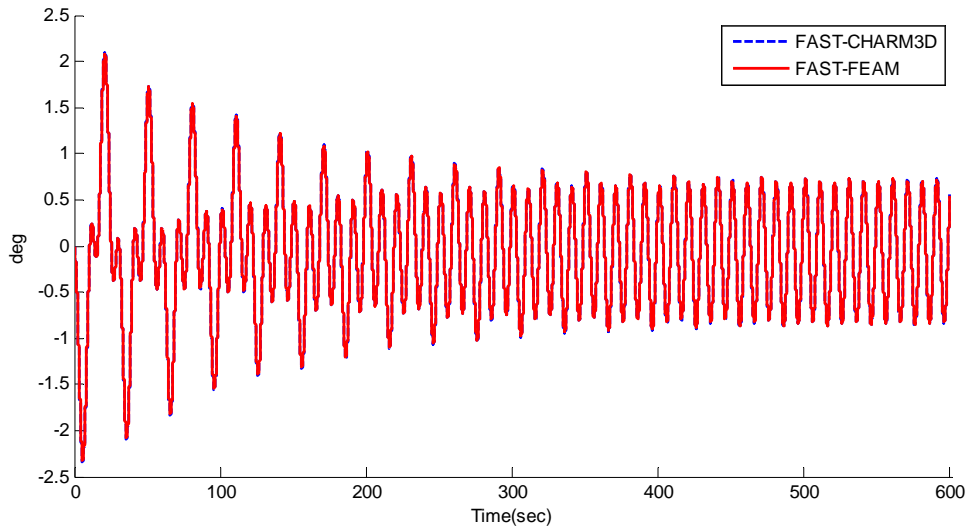**Figure 11. Platform heave with regular wave**

Figure 12. Platform pitch with regular wave

Figs. 10~12 represent the surge, heave and pitch responses of the platform with a regular wave. Except for the slight difference in initial transient heave, all the responses show good agreement.
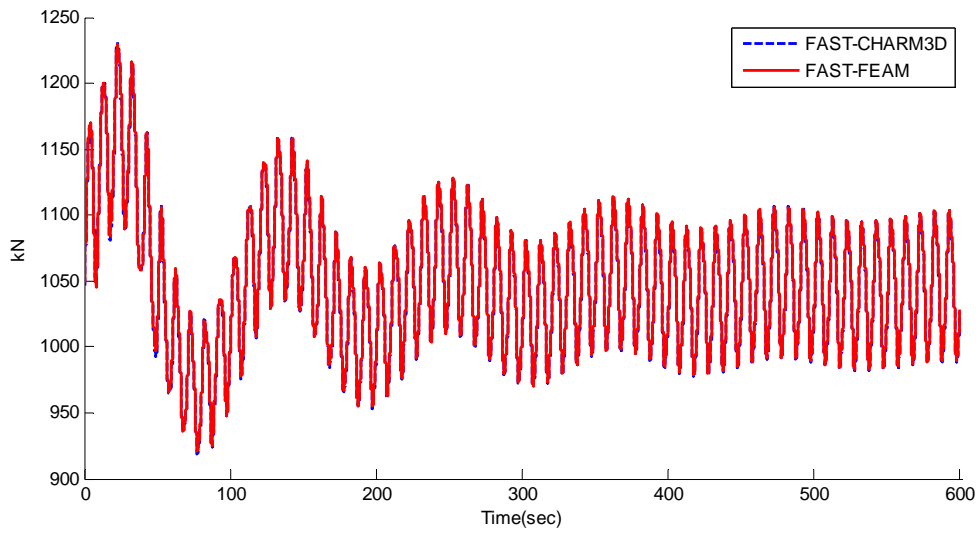

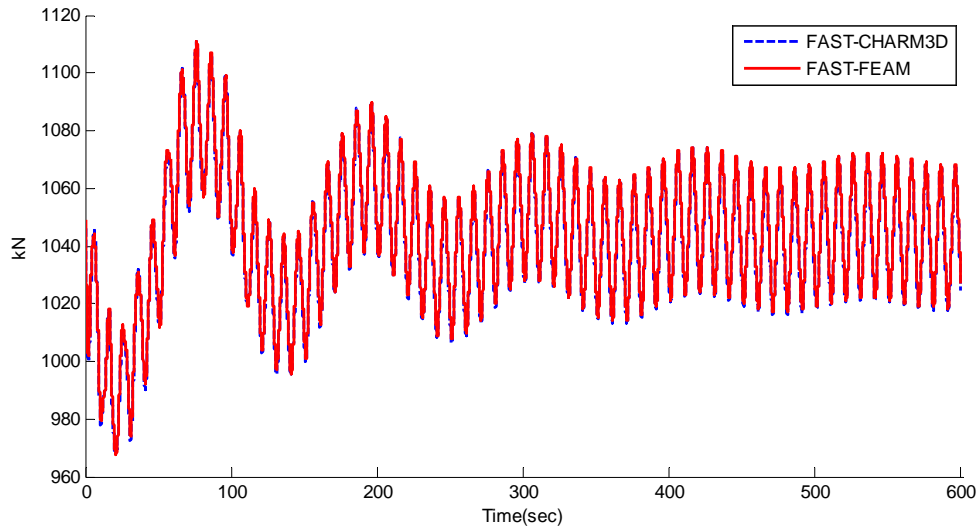**Figure 13. Top tension of the mooring line #1 with regular wave**

Figure 14. Top tension of the mooring line #2 with regular wave
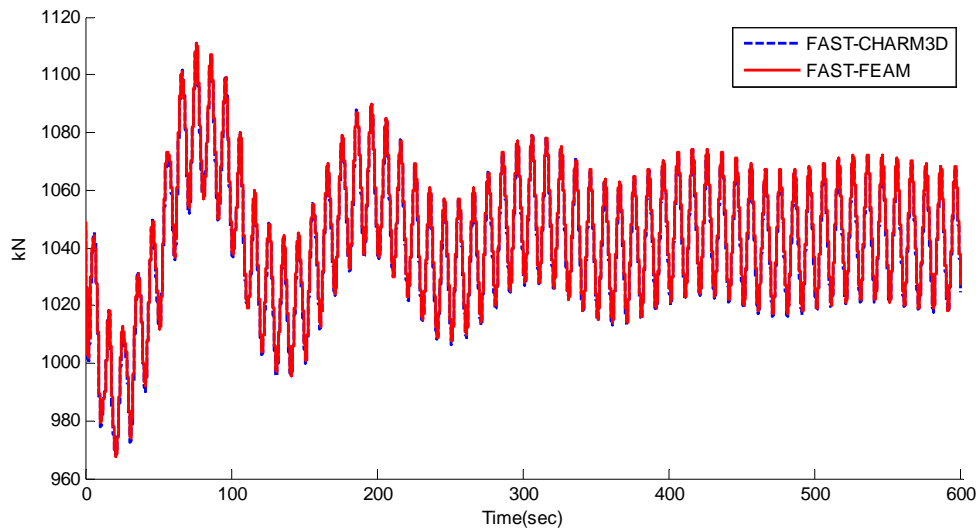

Figure 15. Top tension of the mooring line #3 with regular wave

In the case of the line tensions in Figs.13~15, the time histories show very good agreement between FAST-CHARM3D and FAST-FEAM, which means that all the line dynamics are correctly simulated in the two independent programs. The detail data is additionally attached as an Excel spreadsheet.

7. Conclusion

In this report, the theory of the rod and its finite element model were explained. As a FEAM submodule for the FAST v8, the development work has been done based on the rod theory. The input file format of FEAM module was explained in this report and one example file for OC3-Hywind spar platform was provided. The hydrodynamic loadings on the line element were calculated based on the wave kinematics of the initial position of the mooring lines. The inertia and drag forces of the line elements were computed at every time step and included in the simulation. Free decay test using OC3-Hywind spar platform has been conducted and compared with the result from the independently developed FASTv7-CHARM3D, the FE mooring code incorporated with the FASTv7. The comparison data including platform motion and mooring line tension showed good agreement. The effect of the inertia and drag forces of the line element was also checked and presented. This effect should be considered for the analysis of the deep-water moored platform dynamics. In addition to the free decay test, regular wave test was also conducted. It was confirmed that the platform motions and mooring line tensions using FEAM module were very reliable with incident wave environment.

The newly developed FEAM module can analyze any kinds of mooring lines including catenary mooring, taut mooring, vertical tendons, etc. provided that the proper line geometry and properties are made.